DALTON PERSPECTIVE

Diverse solid-state clusters with strong metal–metal bonding. In praise of synthesis *

John D. Corbett

Department of Chemistry and Ames Laboratory-DOE, Iowa State University, Ames, IA 50011, USA

The synthesis, structure and bonding of two types of metal clusters are described. A large family of zirconium cluster halides of the general type $A^{I}_{x}Zr_6(Z)X_{12+n}$ are obtained with A = Na to Cs, X = Cl, Br or I, $0 < x$, $n \leqslant 6$, and the required interstitial Z atom as variables. Extension to the rare-earth elements (Sc, Y, lanthanides) gives some new, hypostoichiometric cluster variations as well as condensed oligomeric and infinite-chain compounds. Zintl-phase concepts and the alkali-metal compounds that contain anionic 'naked' clusters or cluster networks of the triel elements Ga, In and Tl are also covered. The clusters include empty hypoelectronic examples as well as those that are centred by a heterometal or a triel element. The last compounds are remarkable parallels of the interstitial halides described.

A marked increase in both the interest and research activity in solid-state chemistry has been evident over the past decade. One important aspect of this has been, and continues to be, the search for new compounds and, therewith, a better understanding of the solid state as well as prospects for new or unusual properties and new phenomena. The flow of surprising discoveries makes it clear that our knowledge in many areas of solid-state chemistry, that is what is possible chemically and in structure and bonding, is very incomplete. There is also a great lack of understanding regarding the coupling between structure and physical properties, while the prediction of phase stability among a collection of clear alternatives remains one of the great challenges in science.

The lack of a firm descriptive base in a great many systems, one from which one might rationally extrapolate a chemistry, means that synthesis is often an *exploration* in the real sense of the word. This alone can provide considerable incentive, since the discovery of the totally unexpected, even the hitherto unimagined, is certainly one of the greatest delights in the synthetic exploration of new territory. The best discoveries in an unprincipled area are often those that one stumbles upon during experiments designed with plausible but incorrect or naive ideas regarding possible compounds or structural targets. There are still many new things to be discovered just for the looking.

On the other hand, solid-state products may seem to afford an appreciable downside as far as the purification and characterization methods available to the investigator. Solid-state compounds are for our purposes those with compositions, structures, bonding and properties that are unique to the solid state and semi-infinite in some or all aspects. Means of purification *via* the gas phase or solutions are generally not available, and identification and characterization of such compounds usually must forego most of the methods and the sensitive instrumental techniques that are so well developed for the world of independent molecules or ions. Powder or single-crystal X-ray studies or both are a common route to the identification and characterization of new solid-state products.

Clustering *via* metal–metal bonding is a common property of transition-metal systems when (*a*) the proportion of the accompanying non-metal falls well below that needed for the preferred co-ordination number of the metal, six for example, (*b*) the transition metals lie fairly early in their periods so that the d orbitals are relatively large, and (*c*) some valence electrons remain for metal–metal bonding. This is a long known aspect of niobium and tantalum halide chemistry.[1,2] At a fixed electron count per metal, the clustering is unusually more distinctive with more halide rather than fewer chalcogenide or pnictide (Group 15) anions, the latter giving more condensed and complex structures. Continued metal clustering and condensation in one, two or three dimensions naturally raises the number of near-neighbour metal atoms toward the 12 present in the cubic close-packed (c.c.p.) or hexagonal close-packed (h.c.p.) metals themselves. The contrasting clustering of main-group elements, often in anions or the equivalent, occurs *via* free valencies and many fewer orbitals, often primarily p-type. The borane(2−) clusters often provide the closest analogies.

This Perspective will describe two areas in which relatively recent synthetic explorations, to an appreciable degree in the author's group, have revealed markedly new kinds of cluster chemistry, structures and bonding. One involves halides of the electron-poorer early transition metals, initially for zirconium and then to include the neighbouring rare-earth elements (lanthanides plus Sc, Y) for X = Cl, Br or I. The added electrons and central bonding afforded by an interstitial element within every cluster turns out to be vital to the stability of this family of clusters. Small oligomers are also realized with Group 3 elements, and these naturally blend into infinite condensed products. The related chemistries of Ti and Hf have so far been rather sparse, and relatively little has been reported recently for clusters of the following elements Nb, Ta and Mo save for oxide clusters.[3] None of the latter requires, or apparently allows, that the clusters be centred (except for $[Nb_6I_{11}H]^{0,1-}$).

The second area of new solid-state cluster chemistry is associated with 'naked' (ligand-free) clusters of the heavier triel elements (Ga, In, Tl). Previously homoatomic examples for the post-transition elements concerned electron-richer examples that follow classical skeletal electron counting for deltahedra, M_4^{4-} in many solid AM compounds (Zintl phases) where A = Na to Cs, M (tetrel element) = Si to Pb,[4] or what have been called Zintl ions isolated from molecular solvents with large crypt-alkali-metal cations, Sb_7^{3-}, Bi_4^{2-}, Pb_5^{2-}, Sn_9^{4-}, for instance.[5] The electron-poorer triel analogues exhibit several new ways to achieve surprisingly stable, closed-shell clusters. Again, both of the cluster areas

* Basis of the presentation given at Dalton Discussion No. 1, 3rd–5th January 1996, University of Southampton, UK.

Non-SI unit employed: eV ≈ 1.60 × 10^{-19} J.

that will be described were discovered accidentally while looking for other 'reasonable' species or phases. Gold is still where you find it, and it is not found without looking. (H. J. Emeléus' explanation as to how his laboratory produced many new compounds is apt: as in trout fishing, 'you have to keep a line in the water'.*) Exploratory synthesis should not be too constrained by prior example, experience or 'intuition', and consideration and characterization of the products of even what seem to be failures (according to some plan) can be very worthwhile.

First comes the Synthesis

The results to follow of course represent success in the venture that must come first, the syntheses. The literature provides plenty of examples in which the synthesis and characterization were lacking because of impurities, incomplete reactions, misidentified or missed elements, or misrefined structures as well as cases in which novel phases have been missed because of a lack of exploration of composition or temperature space. The methods and problems of solid-state synthesis have been considered in detail elsewhere,[6] and only a few generalities pertinent to the syntheses of the present clusters will be noted. Kinetically controlled routes to these phases are as yet substantially unknown, a major deficiency, and syntheses under equilibrium conditions are necessary instead. This means that more or less elevated temperatures are used both to overcome characteristic solid–solid nucleation and self-diffusion barriers and, usually, to grow monocrystals suitable for X-ray diffraction.

High-temperature solvents, generally molten salts, have received limited application when the products sought are not sufficiently stable for removal of the solvent by washing since one is otherwise left with a mixture, although excellent crystals may still be secured. Thus, reactions are often run 'neat' with careful control of impurities. This procedure allows a valuable check on assigned compositions too, free of errors from the less-discriminating aspects of X-ray refinement, because of the expectation of a virtually quantitative synthesis from a reaction loaded with the correct composition. (The phase rule works.) This is particularly useful when mixed occupancy of certain sites is not clear or when unrecognized impurity atoms, light ones especially (H, C, N, O), uniquely stabilize a phase and lead to, at best, low and irregular yields until the problem is unravelled. Careful powder pattern and optical examinations as a function of composition alone may allow one to fix the proportions of all elements in a phase within 5–10%.

The early transition metals themselves form such stable binary compounds with C, N, O, Al, Si, Pt, Au, *etc.*, that the use of common elemental or compound containers for their reactions under reducing conditions is generally unsatisfactory above ≈600 °C. Most neat syntheses require 650–900 °C for a week or two. Welded tantalum is a strong and completely inert container under these conditions for zirconium and hafnium systems, while the less costly niobium seems fine for the trivalent and earlier transition elements. Crystal growth in many of these systems probably takes place *via* autogenous transport reactions. In contrast, clusters of the early p-block elements can usually be obtained for their alkali-metal salts directly from the melts (alloys) on cooling, or after intermediate annealing if the phases sought are incongruently melting. The systems are fairly low melting (300–600 °C), and Ta or Nb seem to be perfect as containers. Fused silica would probably also do for systems in which the alkali-metal activity is low and the target is already known.

* American Chemical Society Award Address, Distinguished Service in the Advancement of Inorganic Chemistry, Anaheim, CA, March 1978.

Centred Cluster Halides

The Groups 3 and 4 elements have the right sizes and, when augmented with an interstitial Z, sufficient electron count and bonding to form clusters of the M_6X_{12} type, namely, metal octahedra insulated from their environment by two-bonded inner halide X^i that always bridge all edges. These are evidently stable only when centred by one of a sizeable number of interstitial heteroelements Z, at least for phases prepared under equilibrium (high-temperature) conditions. [Even surface 'interstitials' and room-temperature kinetic routes need to be included in that statement when Z = H, *i.e.* in $Th_6Br_{15}H_7$[7] and $Zr_6Cl_{12}H_x(PR_3)_6$,[8] respectively.] In addition, further outer halide atoms X^a (or other ligands) are always bonded to, and sometimes bridge between, metal vertices on the clusters, additional strongly bonding sites as well. The surprising variety of modes for these interconnections will be considered shortly.

The cluster compounds formed by zirconium (titanium and hafnium) and those obtained with the rare-earth elements (R) form almost exclusive classes. The large number of $Zr_6X_{12+n}Z$ compounds contain halide-bridged network structures constructed from individual clusters, and evidently only a limited number of these cluster types may be centred by 3d transition metals. On the contrary, ternary rare-earth-metal halide phases with isolated clusters exist in only three structure types with, befitting their fewer valence electrons, metal-richer stoichiometries than $R_6X_{12}Z$. There are also a few more conventional quaternary alkali-metal phases, but only one of these is a clear variation on zirconium chemistry. (Although Z is systematically listed last in most formulas, it is always located within the Zr_6 or R_6 framework.) All other products contain clusters condensed *via* shared metal edges into chains that are still sheathed by halide bonded at exposed cluster edges and vertices. A pleasant surprise on the way to these chains is the occurrence of an appreciable number of stable oligomers. The R-based cluster phases in general encapsulate a variety of later 3d, 4d and 5d elements as interstitials.

In terms of background, the zirconium cluster halide principles and many examples were described fairly thoroughly in 1989[9] and in a 1992 overview of mainly the crystallographic and structural aspects.[10] Rare-earth-metal halide systems in oxidation states below two were covered in a thorough fashion in a review by Simon *et al.*[11] for the literature through 1988 plus some from 1989. Notice of nearly all of the R-rich cluster, oligomer, and chain phases with transition-metal interstitials has appeared since then. Both families of cluster halides were included in a recent overview.[12] Finally, although these will not be considered further, the existence of a few truly *binary*, condensed cluster phases for these elements (without Z) is worth noting: (*a*) the double-metal-layered ZrCl and ZrBr which have a modest interstitial chemistry, (*b*) the original discovery in this area, Gd_2Cl_3 and the related Sc_7Cl_{10},[13] both constructed from face-capped (M_6X_8-type) clusters condensed into chains, and (*c*) the recently discovered NiAs-type LaI.[14]

Zirconium cluster systems

The combination of basic $Zr_6X_{12}Z$ clusters with *exo* bonding generates a great variety of structures and compositions that with virtually no exceptions fit into the general description $A^I_x[Zr_6(Z)X^i_{12}]X^a_n$ in which x, Z and n are variables. Thus $0 \leqslant n \leqslant 6$ additional halides may be used to fulfil some or all of the bonding required at each vertex on the centred 6–12 cores, Fig. 1, and these variations have major structural impacts. In addition, x alkali-metal (occasionally alkaline-earth-metal) cations, A, may be accommodated within halide-bounded cavities, presently over the range $0 \leqslant x \leqslant 6$. The need for these cations is driven electronically by the choice of Z and the magnitude of n. As far as the n dependence, isolated clusters are naturally obtained for $Zr_6(Z)X^i_{12}X^a_6$ (= $Zr_6Cl_{18}Z$)

with one-bonded X^a at each vertex. Somewhat less X (smaller n) means some of these outer halides must become bridging X^{a-a}, and this continues to the composition $Zr_6(Z)X^i{}_{12}X^{a-a}{}_{6/2}$ (= $Zr_6Cl_{15}Z$) where all vertices are so bridged. Still smaller n values require that some inner bridging X^i now must also bond at vertices in other clusters, *i.e.* as three-co-ordinate X^{i-a} (and X^{a-i}). At the present lower limit (n = 0), half of the inner edge-bridging X^i double up as X^{i-a} to give $Zr_6(Z)X^i{}_6X^{i-a}{}_6$ (= $Zr_6X_{12}Z$). The regular way in which bridging in the last is accomplished (with Z = H, Be, B or C) is shown in a [110] section in Fig. 2.[15] The three-dimensional import is clearer when it is realized that the centred Z (crossed ellipsoids) all lie on both a vertical three-fold axis and an inversion centre. Conversely, the progression through compounds with increasing n in principle occurs structurally by successive conversion of the bridging functions from X^{i-a} into X^{a-a} into X^a, the order of decreasing co-ordination number and increasing basicity. Other factors may intercede, however; the first example discovered for a 6–13 proportion was the exceptional $Zr_6(B)Cl^i{}_{10}Cl^{i-i}{}_{2/2}$-$Cl^{a-a-a}{}_{6/3}$ with two other halide functionalities, one that is *trans*-edge-bridging in two clusters (i-i) to generate chains and another that bonds to three vertices in adjoining chains (a-a-a).[16] Fig. 3 shows just these bridging halides in a recent tetragonal example, $Zr_6(B)Cl_{11.5}I_{1.5}$ (the iodine mixes only on X^i sites).[17] Clearly the sizes of the halogen and Z, the sizes and numbers of any cations, and space-filling efficiency also have influences on the structures chosen.

These last aspects are seen especially well in the considerable structural variety secured with n = 3, that is for $Zr_6(Z)$-$X^i{}_{12}(X^{a-a})_{6/2}$. The simple arrangement in cubic $[Zr_6(Co)$-$Cl_{12}]Cl_{6/2}$ shown in Fig. 4[18] (with the 12 Cl^i atoms omitted from each cluster for clarity) is based on two primitive $ReO_{6/2}$ lattices in which clusters have replaced Re atoms. This network is proportioned so that two nets in a body-centred cubic (b.c.c.) arrangement can now interpenetrate without any interconnections. Nothing larger than Li^+ can be accommodated in the annuli, *e.g.* in $Li_2Zr_6(Mn)Cl_{15}$. Five more independent ways of cluster interconnection for 6–15 compositions have been found, arrangements that cannot be interconverted without bond breakage.[19] One cubic member, $Zr_6(N)Cl_{15}$, requires a small interstitial and, in addition, only a small amount of sodium counter cation can be accommodated when the interstitial is changed to carbon. One or two larger cations can be bound in a third version, $KZr_6(C)Cl_{15}$ and $CsKZr_6(B)Cl_{15}$. (Note the electronic compensation between the number of cations and the Z electron count present in the previous Co, Mn pair and for the last three with Z = N, C or B. This aspect will be pursued shortly.)

The versatility provided by the several variables in these zirconium systems, particularly regarding size, charge and electronics, happily provides many examples (as above) of structural motifs that could never have been foreseen. A novel variation on the structure just shown is found for $Cs_3(ZrCl_5)Zr_6(Mn)Cl_{15}$[20] wherein the network portion, Fig. 5, derives from a primitive ReO_3-like [or half of the cubic

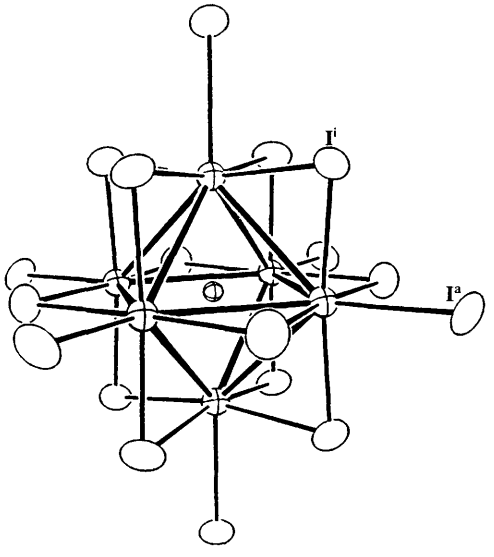

Fig. 1 A $Zr_6(Z)X_{12}$ cluster unit with six additional X^a halide atoms at the cluster vertices (Zr and the centred interstitial Z are drawn with crossed ellipsoids)

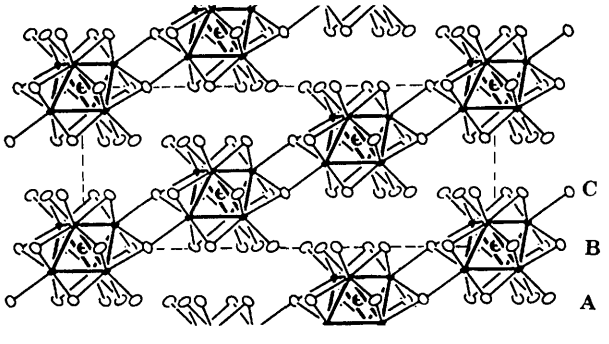

Fig. 2 A [110] section of rhombohedral $Zr_6X_{12}Be$ with the $\bar{3}$ clusters linked by six X^{i-a} bridges about the cluster waists (the Be atom is crossed and the Zr atoms are connected by heavier lines; $\vec{c}$ is vertical). The halide layers, A, B, C are close packed

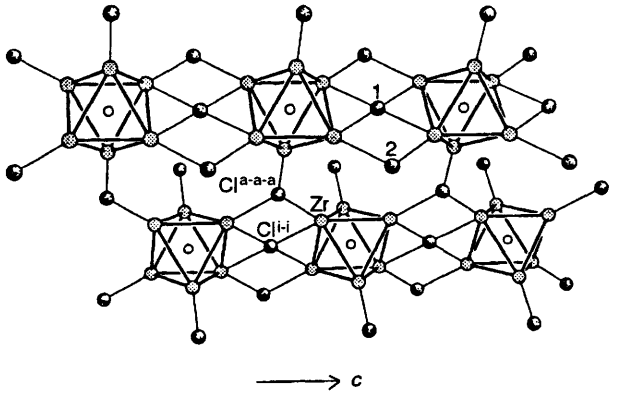

Fig. 3 Novel chlorine bridging functions within the tetragonal structure of $Zr_6BCl_{11.5}I_{1.5}$. The Zr_6 units are outlined, but with their edge-bridging Cl, I omitted. Note the *trans*-Cl^{i-i} (1) and Cl^{a-a-a} (2) bridging functions (irregular shaded atoms)

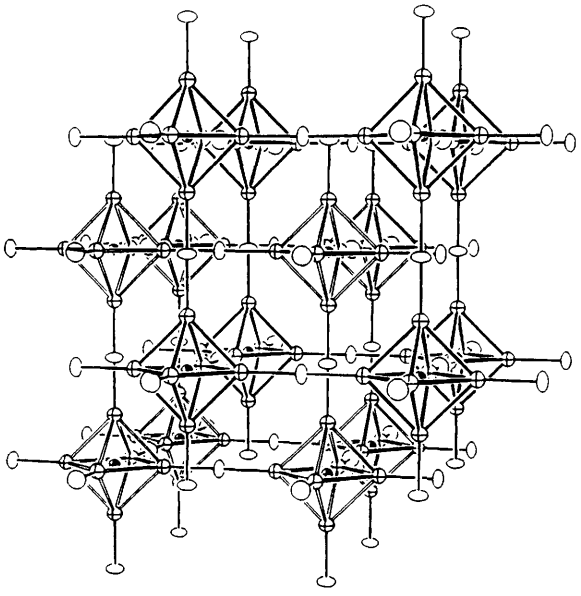

Fig. 4 A portion of the cubic structure of $[Zr_6(Co)Cl^i{}_{12}]Cl^{a-a}{}_{6/2}$ with the Cl^i atoms not shown. Note the two interpenetrating lattices; Cl^{a-a} are open, Zr crossed and Co shaded ellipsoids. Reprinted with permission from ref. 18. Copyright 1991 American Chemical Society

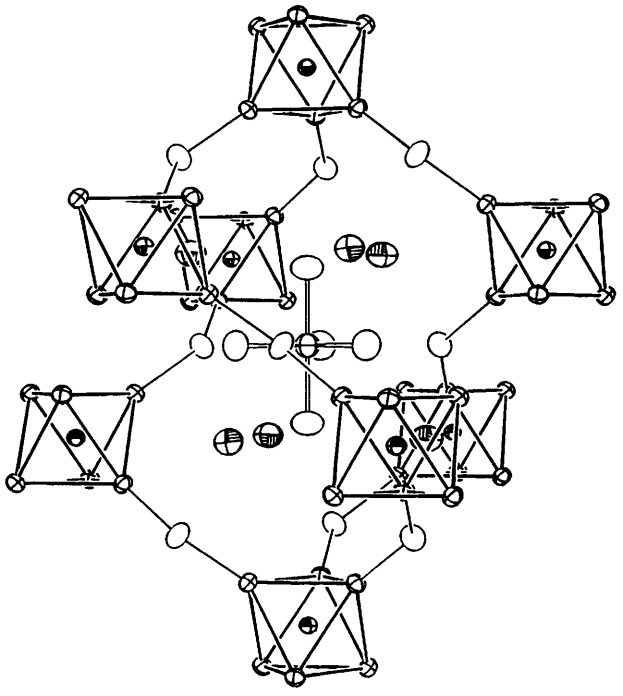

Fig. 5 One cavity in the $[Zr_6(Mn)Cl_{12}]Cl_{6/2}^{2-}$ network (Cl^i omitted) and the $ZrCl_5^-$ and Cs^+ ions therein in $Cs_3(ZrCl_5)Zr_6(Mn)Cl_{15}$. The result is a stuffed rhombohedral perovskite. Reprinted with permission from ref. 20. Copyright 1995 American Chemical Society

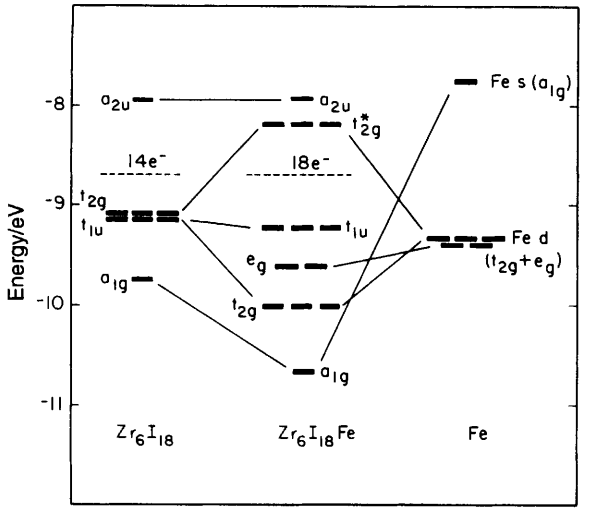

Fig. 6 Molecular orbitals for a $Zr_6I_{12}I_6$ cluster (left) and the results when an iron interstitial (or, qualitatively, another d element) is added. Addition of a main-group Z lowers a_{1g} (s) and t_{1u} (p) instead. The two types of centred clusters have optimal 18 and 14 cluster-based electrons, respectively. Reprinted with permission from ref. 25. Copyright 1988 American Chemical Society

H						Be	B	C	N
							Al	*Si*	*P*
K	*Cr*	Mn	Fe	Co	Ni			*Ge*	

Scheme 1

$Zr_6(Co)Cl_{15}$] network that has undergone a trigonal twist about [111]. The centre of each cavity in this array now traps the novel $ZrCl_5^{2-}$ (D_{3h}) anion, which does not share any halogen with the network. The $(ZrCl_5)[Zr_6(Mn)Cl_{12}](Cl^{a-a})_{6/2}$ components of this structure correspond group-by-group to an $ABX_{6/2}$ rhombohedral perovskite. The cations necessitated by the charges on the first two portions are then 'stuffed' into fairly suitable 12-co-ordinate positions in this otherwise rather open structure. The fit is rather special, and the corresponding caesium boride is the only other member that has been found with this structure. A related bromide without the ZrX_5^- anion is achieved in $Cs_3Zr_6(C)Br_{15}$.[19] Only the caesium cations now fill the central cavity, fractionally distributed over sites that have only three or four bromine near-neighbours. Network structures often demonstrate how particularly the larger, lower-field cations may have to settle for relatively poor, low-symmetry sites with small numbers of halide as neighbours, the dominant structure-making features evidently being associated with the cluster network.[10,21]

The number of compositions that have been achieved for centred zirconium clusters is well over 100. The range of Z possible in one type or another is noteworthy, as in Scheme 1. The italicized Z have so far been encapsulated only in iodides. The structural varieties achieved with iodide clusters are remarkably fewer than for the chlorides, namely only for $n = 0$ or 2 in $Zr_6I_{12}Z$, (Z = H, Be, B, C, Cr or Mn) and for $A_xZr_6I_{14}Z$ (A = Li to Cs; Z = B, C, K, Cr to Co, Al, Si, P or Ge). (There is also a mixed Si–B result obtained when an errant Pyrex chip was reduced![22]) Hafnium chlorides by contrast exhibit a very modest cluster chemistry, all related to that of zirconium and apparently limited to a few carbides and borides,[23] and there is one example of an analogous titanium cluster, $Tl_6(C)Cl_{14}$, prepared near 500 °C by a metallothermic reaction with alkali metal.[24] (Our earlier attempts in the same system by a more traditional route near 550 °C were broadly unsuccessful in producing any useful crystals, although new powder patterns were seen.)

The blank spaces in Scheme 1 should for the main part be taken to mean that those Z have been tried but failed to intercalate. It is difficult to generalize about reasons for these omissions. The syntheses are carried out under equilibrium conditions, so high yields, often >90%, can be expected when the right proportions are loaded. The important aspect for success or failure is not that a particular cluster may be poorly bonded *per se*; rather, *the stability of any compound is always relative to the stabilities of alternative phases*. For successful reactions, the obvious binary alternatives for Z such as ZrC, ZrB_2, Zr_3Fe together with appropriate halide phases (ZrCl, ZrX_3, A_2ZrX_6, *etc.*) must be less stable.

Bonding in $M_6X_{12}Z$-type clusters

All theoretical treatments of nominally octahedral M_6X_{12} clusters, however modified these may be chemically, give much the same results in terms of M–M bonding and HOMO (highest-occupied molecular orbital) descriptions, basically because of symmetry. (It is important, however, to include *exo*-halides, as in an $M_6X_{12}X_6$ arrangement, as these lie *trans* to the M–Z bonding interactions.[15]) The introduction of a centred interstitial hydrogen, main-group element, or transition metal adds one (s), four (s,p) or six (d,s) more good orbitals and, importantly, some additional electrons to the problem, but the orbitals introduce no new bonding states to the cluster-based levels/representations. The general ideas can be deduced from Fig. 6.[25] On the left is a typical result, for $Zr_6I_{12}I_6$ in this case, in which the most strongly bonding and principally zirconium-based levels a_{1g}, t_{1u} and t_{2g} define a 14-electron cluster-based limit. (Iodine levels all lie lower.) The gap to a_{2u} depends on, among other things, some relative dimensions of the cluster (below). Clearly, s and p valence levels (not shown) of a main group atom Z, which usually lie somewhat lower, mix with and lower the a_{1g} and t_{1u} cluster levels appreciably, the corresponding added levels being high-lying a_{1g}^* and t_{1u}^*. Thus, the usual cluster-based bonding orbitals hold 14 electrons, the foregoing a_{1g}^2 and t_{1u}^6 plus t_{2g}^6 which is bonding

solely within the cluster shell, with or without a centred main-group element. Of course, hydrogen lowers only the a_{1g} level, presuming it is centred. Hypervalency descriptors for these centred clusters seem unnatural and unnecessary.

A centred d-element interstitial alters this picture in a fairly obvious way, as shown on the right of Fig. 6. A major difference is that the e_g^4 valence levels on these Z have no counterpart among the lower-lying, cluster-bonding orbitals and remain localized on Z. Thus, only t_{2g} (d) and a_{1g} (s) thereon mix appreciably with Zr–Zr bonding levels, while t_{1u}^6 now is just M–M bonding since p orbitals on transition metals generally lie too high to be effective. Since the difference between 14 and 18 electrons for closed shells with the two types of Z arises because of e_g^4 in the latter, pairs of interstitials like B and Mn, or C and Fe, are isoelectronic in their contributions to cluster bonding, a novel circumstance.[26]

These guidelines have proven to be especially valid for the zirconium chlorides, where there are only a few exceptions to the 14- or 18-electron 'rules' and a wide range of structures are available. This means compositions and structures can often be systematically generated or synthetically 'forced' by the Z provided, often in concert with the amount of ACl. For instance, known phases with fixed n include $Zr_6Cl_{15}N$, $KZr_6Cl_{15}C$, $K_2Zr_6Cl_{15}B$ and $K_3Zr_6Cl_{15}Be$, and with fixed Z instead, $RbZr_6Cl_{14}B$, $Rb_2Zr_6Cl_{15}B$, $Rb_3Zr_6Cl_{16}B$ and $Rb_5Zr_6Cl_{18}B$. A majority of the exceptions to 14 electrons in chlorides is for hydrides (something seems to be better than nothing) in phases in which Be would give the optimal 14. Iodides are less 'faithful', variants including 16 in the very stable $Zr_6I_{12}C$ and 15 in $AZr_6I_{14}C$ and $Zr_6I_{12}B$.

Explanations for clusters stable with > 14 e have fairly wide applicability and are based on *matrix effects*, namely the alteration of distances, angles and bonding that result from closed-shell contacts, often between halogen atoms.[10,27] Thus there may be a dimensional conflict between optimal $M_6(Z)$ cluster size and the surrounding $12X^i$. The edge-centred cube defined by X^i (Fig. 1) is usually larger than that for M_6 vertices because of close X···X contacts, which cause the metal vertices to lie inside the faces of the cube. This is exacerbated by large halide (I > Br > Cl), small M (Nb > Zr), and small Z (C, N, *etc.*). It also means that the approach of X^a to a good bonding distance from a vertex may be limited by its contacts with the four neighbouring X^i.[25] The correlation between cluster distortions and electronic deviations originates with the character of the a_{2u} LUMO (lowest unoccupied molecular orbital) (Fig. 6), which is M–M bonding but M–X^i π antibonding. Withdrawal of metal vertices from the X^i plane reduce the π* component and the a_{2u} level falls. Its occupation in 15- and 16-electron species is therefore favoured for large X, small M and, of course, small Z, as observed. This behaviour seems widely observed;[9,10,19,28] both centred (Zr) and empty (Nb, Ta) halide clusters appear to follow it even though the totality of bonding interactions in the two types, centred and not, differs appreciably.

Another widely applicable matrix effect is shown by the M–M distances in centred clusters, which are principally determined by d(M–Z) and not by M–M bonding. Cluster sizes frequently parallel those conventionally assigned to the interstitial 'props'. At the extreme, Z = N or H in zirconium chlorides yields the minimum cluster size that must be defined principally by Zr–Zr interactions. The zirconium–cluster midpoint distances in $K_2ZrCl_6{\cdot}Zr_6Cl_{12}H$[29] and $Li_6Zr_6Cl_{18}H$[30] are 2.26 Å, about 0.16 Å greater than expected for good Zr–H bonding on the basis of the dimensions of other phases. The implied 'rattling' of hydrogen has been confirmed both by the relaxation characteristics of ^1H in the NMR spectrum of $Zr_6Cl_{12}H$ at room temperature[31] and by an inelastic neutron scattering study of vibration modes in $Li_6Zr_6Cl_{18}(H,D)$ at 15 K, where the deuteron appears bound in a μ_3 manner on an (internal) triangular face of the cluster.[32]

H						B	C	N
							Si	
	Mn	Fe	Co	Ni	Cu			
		Ru	Rh	Pd				
	Re	Os	Ir	Pt	Au			

Scheme 2

Solution reactions

In principle it should be possible to treat halide-bridged cluster structures with suitable nucleophilic ligands so as to dissolve the clusters in non-aqueous solvents, corresponding to a bridge-opening step like $[Zr_6(Z)\text{–}X\text{–}Zr_6(Z)] + L \longrightarrow Zr_6(Z)X^- + Zr_6(Z)L$. This could lead to new substitution derivatives, new salts and, perhaps, new extended solids. Some success has been had with certain structure types, *e.g.* equation (1), as well as in

$$KZr_6Cl_{15}Fe(s) \xrightarrow[NEt_4Cl]{MeCN} [NEt_4]_4[\{Zr_6(Fe)Cl_{12}\}Cl_6] + KCl \quad (1)$$

the generation of neutral clusters such as $Zr_6Cl_{12}H(PR_3)_6$.[33] This chemistry has been carried a good deal further by Hughbanks and co-workers[34] in room-temperature molten (chloroaluminate) solvents, which also allow the utilization of more strongly interlinked substrates.

Rare-earth-metal phases

These elements provide a virtually unique cluster chemistry relative to that for zirconium and hafnium. The reduced number of valence electrons is doubtlessly a major factor. Only a few isolated clusters occur, either in ternary compounds or in quaternaries with appropriately large x and small n, while the remainder of the reduced halides (X:R < 2:1) exhibit cluster condensation, usually through shared edges, into either oligomers or chains. All discrete clusters contain interstitials, and all of the ternaries are hypostoichiometric relative to M_6X_{12} compositions. Many of the novelties occur with iodides, while chlorides are relatively sparse in new chemistry. The variety of interstitials that have been bound is larger and somewhat different than before (Scheme 2). The d-element boundaries are fairly well established, at least for prototypical compositions, but not all R have been sampled, and there are some trends in stabilities with R that may extend to Z.

Discrete clusters

The three discrete cluster structures without low-valent cations are rhombohedral $R_7X_{12}Z$ and triclinic $R_6I_{10}Z$ and $R_{12}I_{17}Z_2$. The $R_7X_{12}Z$ structure, first described for Sc_7Cl_{12} in 1978 without an identified interstitial, is derived from that of $Zr_6X_{12}Z$, Fig. 2, by insertion of a seventh oxidized (R^{III}) metal in the antiprismatic cavity that lies midway between clusters along the $\bar{3}$ axis (z). The seventh R atom naturally serves to raise the cluster-bonding electron count.

The reduced halogen content in the parent $Y_6I_{10}Ru$[35] is accomplished with a pair of $X^{i\text{-}i}$ atoms that bridge edges in adjoining clusters and parallel a pair of conventional $X^{i\text{-}a}$ functions per cluster. A portion of the chain created is shown in Fig. 7 for $Pr_6Br_{10}Ru$.[36] Systematic syntheses of these phases for R = Y, Pr or Gd with a large range of transition-metal Z demonstrate the breadth of this chemistry and how widely the cluster electron counts may vary. Fig. 8 illustrates this with cell volume data *vs.* the Group of Z, Period by Period, for $R_7I_{12}Z$ compounds of Pr, Gd and Y (top) and for $Y_6I_{10}Z$ examples (bottom).[37] The cluster electron counts are given at the top of

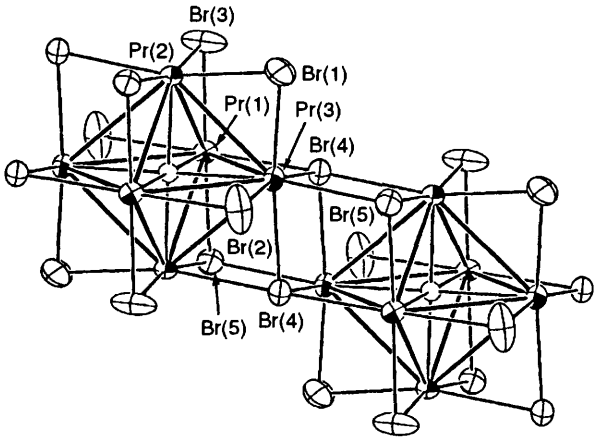

Fig. 7 One segment of the unique chains of clusters in $Pr_6Br_{10}Ru$. Note the pairs of $Br(4)^{i\text{-}i}$ and $Br(5)^{i\text{-}a}$ bridges (unbonded vertices are actually $Br^{a\text{-}i}$ bridged from other chains). Reprinted with permission from ref. 36. Copyright 1994 American Chemical Society

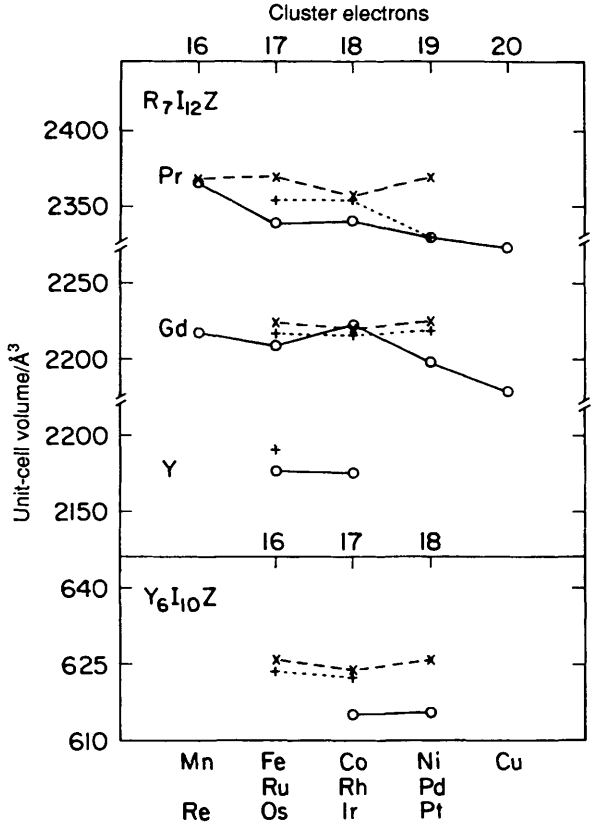

Fig. 8 Cell volume *vs.* Group of the interstitial for $R_7I_{12}Z$ (R = Pr, Gd or Y) (top) and $Y_6I_{10}Z$ (bottom) phases. The 3d, 4d and 5d elements Z are marked by ○, + and ×, respectively. The cluster-based electron counts are shown above each section. Reprinted with permission from ref. 37. Copyright 1990 American Chemical Society

each section. As many as five consecutive 3d, or four 5d, elements can be encapsulated in certain hosts. The surprising 18 ± 2 range of cluster counts may derive from the greater polarity of R–X (compared with Zr–X) and, in some cases, because of the lower-lying valence levels of the late, heavy transition metal Z. The 16-electron $Pr_6Br_{10}Ru$ depicted in Fig. 7 actually exhibits a 0.276 Å (9.8%) decrease in the vertical *d*(Pr–Ru), an apparent Jahn–Teller distortion from a t_{1u}^4 HOMO in the octahedral cluster. An unusually low I : R ratio is achieved with only discrete clusters in $Pr_{12}I_{17}Z_2$ (Z = Fe or Re) by means of seven $I^{i\text{-}i}$ bridges per cluster in a relatively complex structure.[38] The average cluster in these contains 17.5

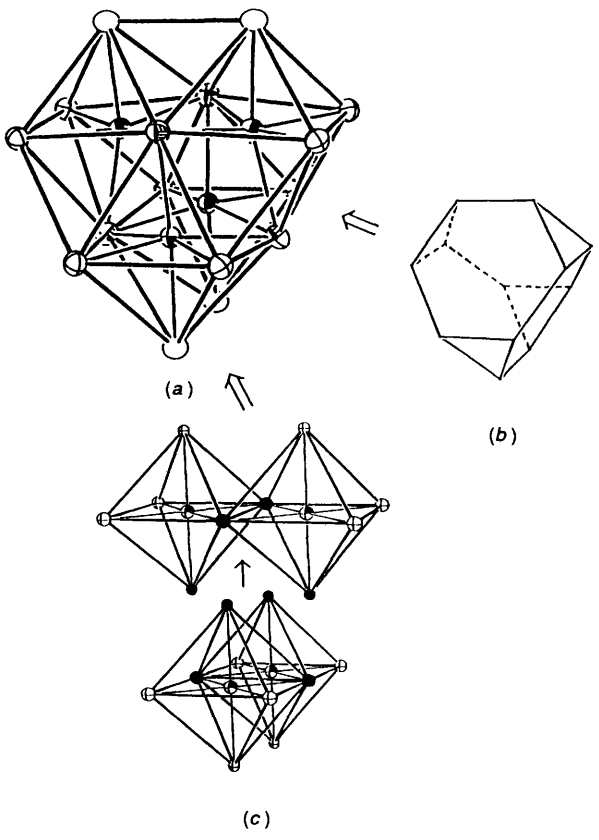

Fig. 9 The construction of (*a*) an $R_{16}Z_4$ cluster from (*b*) a truncated tetrahedron R_{12} with capping of the four hexagonal faces and insertion of a Z_4 tetrahedron or by (*c*) a 2 + 2 condensation of R_6Z clusters

electrons, but there is no evidence for different clusters in the structure at room temperature.

Cluster condensation

A proliferation of new phases, beyond the discrete cluster iodides above, is found for well reduced combinations of scandium, yttrium or a lanthanide element, iodine (or in some cases, bromine) and, in particular, a transition metal Z. Most relevant is a surprising group of tetrameric bromide and iodide oligomers that show well defined electronic stabilities. All types can be generated conceptually through sharing two or more R–R edges between octahedra, a process generally controlled by the X : R ratio.

Oligomers. Table 1 summarizes the four oligomer structure types according to their formulae and space groups. A further description of the components is also included where appropriate, as well as the cluster-based electron counts and magnetic characteristics where known.[39,40] Fig. 9 illustrates the nature of the $R_{16}Z_4$ core structure and its imagined construction from either a tetracapped truncated tetrahedron plus 4 Z or (*c*) a two-by-two condensation of conventional R_6Z clusters. The shared edges of the imagined dimeric precursors, now defined by pairs of the unique R that cap hexagonal faces of the tetrahedron, are considerably (≈20%) longer than the other R–R edges. The parent octahedra in (*c*) have been additionally distorted by movement of Z toward the centre of the new unit, although the Z–Z distances remain large in most cases. The second type of oligomer with a 16–24–4 composition (Table 1) arises when interstitial Ir replaces Ru, the four-electron increase therefrom being simply compensated by the addition of four more bromines to the oligomer sheath with corresponding changes in bridging functions. The pleasures derived from the discovery of new synthetic wonders were once again realized in somewhat YBr_3-richer systems with a third

type, $Y_{20}Br_{36}Ir_4$, where a distinguishable YBr_3 component bridges between oligomers, edge-sharing $Y^{III}Br_{4/2}Br_{2/2}$ octahedra. These are again 60-electron units.

The addition of Cr, Mn, Ni or Pt as interstitials to reduced yttrium bromides gave none of these structure types, as might be expected for electronic reasons. Rather, the smaller scandium bromide host yields yet a fourth type for Z = Fe, Ru or Os in a cubic structure first discovered for gadolinium, $Gd_{20}I_{28}Mn_4$.[41] The latter, Fig. 10, contains a similar oligomeric unit plus a second small cluster in a sphalerite-like hierarchy, a tetrahedral Gd_4I_8 cluster that is iodine-bridged to four oligomers and *vice versa*. The large Gd–Gd separations in the latter lead to the conclusion that this must be a $Gd_4I_8^{4+}$ (Gd^{III}) unit which functions as an electron donor and thereby again affords a 60-electron oligomer. The skeletal electron count of such oligomers would necessarily change by four when the group of Z is altered by one, all else fixed. Thus, the switch to an iron-group interstitial in $Sc_{20}Br_{28}Z_4$ analogues is largely compensated by the omission of precisely one (disordered) metal atom from the small cluster to yield 61-electron units $Sc_{19}Br_{28}Z_4$ (Table 1). Magnetic data for the compounds with Z = Fe, Ru or Os are nicely consistent with one unpaired electron per oligomer. It should be noted that this class of compounds has been found only for the smaller R = Sc, Y or Gd and not with La or Pr. Just the converse applies for both the $R_{12}I_{17}Z_2$ cluster phases (above) and the R_4I_5Z chain compound below.

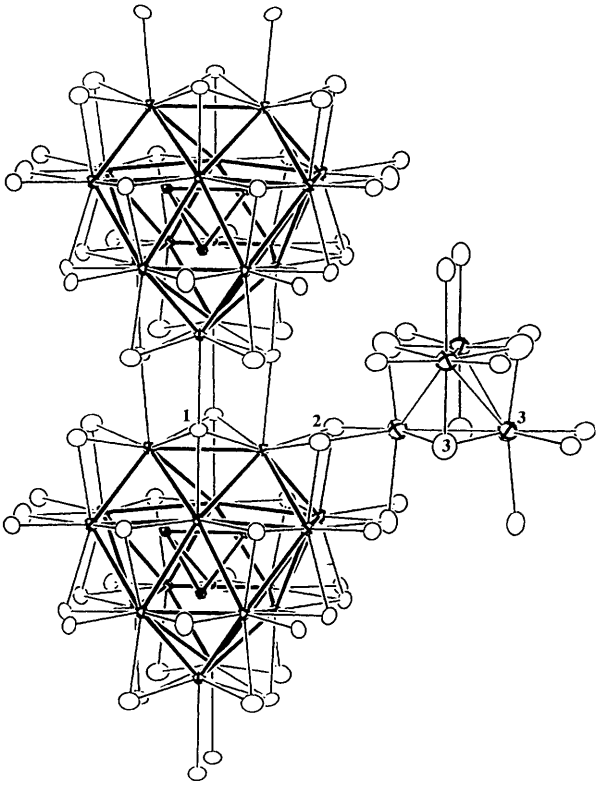

Fig. 10 The twin clusters in cubic $Gd_{20}I_{28}Mn_4$, which are formulated as $Gd_4I_8^{4+}Gd_{16}I_{20}Mn_4^{4-}$ (ellipsoids of Gd are crossed, those of Mn shaded). Reprinted with permission from ref. 41. Copyright 1994 American Chemical Society

Infinite products. The novel condensed chain phases found for a variety of reduced rare-earth-metal iodides are further revelations of a diverse chemistry. Because of the 'cluster' subject matter, only two recent types will be illustrated briefly. (Other sources are more expansive and thorough.[11,12]) These are the monoclinic single-chain R_4I_5Z, and double chain R_3I_3Z which, with Z examples such as Mn, Co, Ru and Os to Au, constitute distinctive and novel one-dimensional 'heterometal nanowires'. Fig. 11 shows a portion of one chain for Pr_4I_5Ru with Pr atoms shaded and Ru as crossed ellipsoids.[42] The octahedral units are characteristically elongated along the chain repeat relative to the shared edge. The four iodines per cluster shown (open ellipsoids) each simultaneously bridge edges of adjoining cluster units (and, in part, bond to praseodymium vertices in other chains), while the fifth I^{i-i} (not shown) is bonded between edges of adjoining chains. As with other isolated (18-e^-) and condensed chain phases of the rare-earth elements, Pr_4I_5Ru shows neither magnetic effects from the interstitial nor significant coupling between the $4f^2$ cores of the framework Pr. The lanthanum analogue exhibits a small temperature-independent paramagnetism appropriate to the Pauli paramagnetism of conduction electrons, consistent with the metallic behaviour predicted by one-dimensional extended-Hückel band calculations. The broad conduction band contains only metal-based states, with Ru making significant contributions mostly near and below E_F (Fermi energy) an interesting and sensible contrast with the band distributions in the isostructural Y_4I_5C where the Pr–C valence band falls 3–4 eV below E_F.[43]

Finally, the [010] view of the unit cell of the same Pr_4I_5Ru along the chain direction in Fig. 12(*a*) is compared with the double-chain construction in Pr_3I_3Ru in Fig. 12(*b*). Here, pairs of the chains seen individually in Pr_4I_5Ru have been displaced from each other by *b*/2 and further condensed through sharing of side edges. Phases of this type with smaller R and other Z

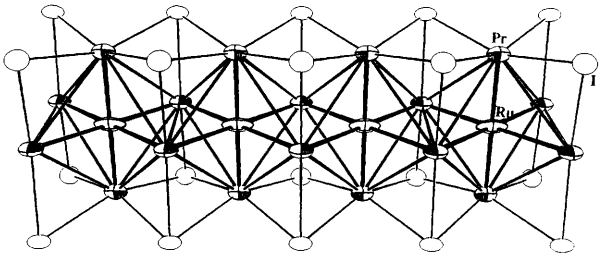

Fig. 11 A side view of the condensed chain in Pr_4I_5Ru. Note the *trans*-edge-sharing $Pr_{4/2}Pr_2(Ru)$ clusters (Pr–Ru bonding emphasized) and the iodines that each bridge two cluster edges (light lines)

Table 1 A family of $R_{16}Z_4$ cluster oligomers[a]

Type	Compounds	Space group	Oligomer electron count	Magnetism[b]
1	$Y_{16}I_{20}Ru_4$,[c] $Y_{16}Br_{20}Ru_4$, $Sc_{16}Br_{20}(Fe,Os)_4$	$P4_2/nmm$	60	t.i.p.
2	$Y_{16}Br_{24}Ir_4$	$Fddd$	60	
3	$Y_{20}Br_{36}Ir_4$ ($Y_{16}Br_{24}Ir_4{\cdot}4YBr_3$)	$I4_1/a$	60	t.i.p.
4	$Gd_{20}I_{28}Mn_4$[d] ($Gd_4I_8^{4+}Gd_{16}I_{20}Mn_4^{4-}$)	$P\bar{4}3m$	60	
	$Sc_{19}Br_{28}(Fe,Ru,Os)_4$		61	CW
	$Sc_3Br_8^+(Sc_{16}Br_{20}Z^-)$			

[a] Ref. 40 except as noted. [b] t.i.p. = Temperature-independent paramagnetism, presumably van Vleck in character; CW = Curie-Weiss behaviour. [c] Ref. 39. [d] Ref. 41.

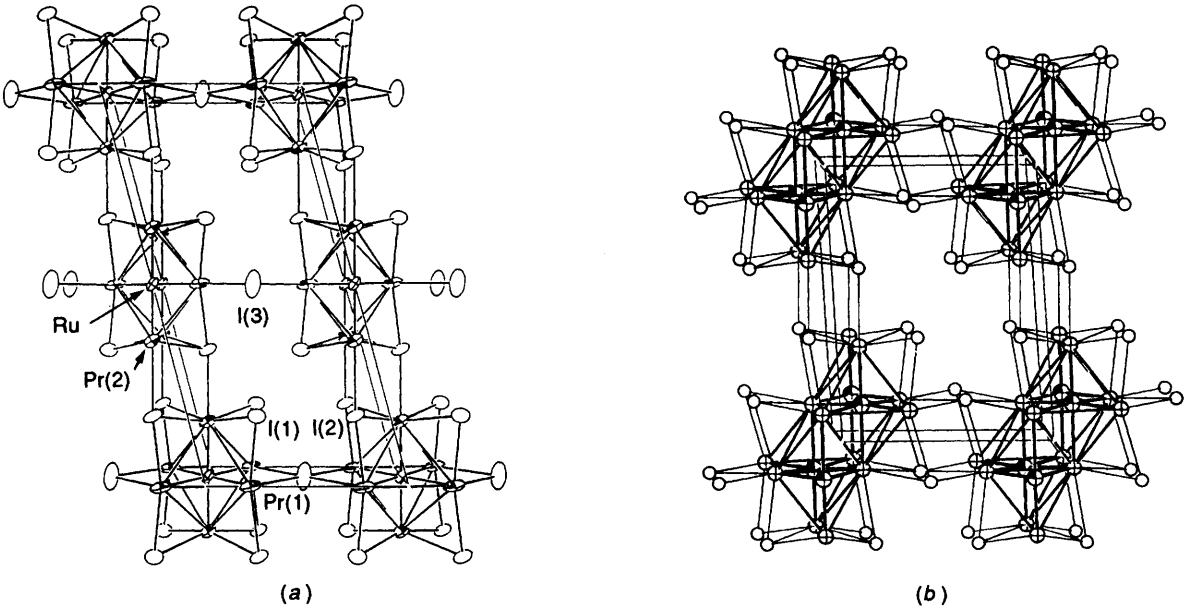

Fig. 12 Projections down (*a*) the condensed single chains in monoclinic Pr_4I_5Ru (Fig. 11) and (*b*) the double chains in monoclinic Pr_3I_3Ru

show unusual distortions as the pairs of chains more-or-less merge into one another, a feature that is not well understood.[44] There are no general rules regarding the electronic stability of the chain compounds, although the Z ranges for each tend to be fairly narrow.

Although the foregoing certainly qualify as unusual when judged from the status of the field 10–15 years ago, one is never prepared for the unprecedented as was recently revealed by the near-singularity of the semiconducting R_4Br_4Os (R = Y or Er) generated from confacial, centred *square-antiprismatic clusters*[45,46] and the NiAs-type metallic LaI.[14]

Zintl Phases

Rather different chemistries and principles apply to naked (ligand-free) clusters of p-block elements. The electron-richer clusters of the tetrel and pnictogen elements noted in the Introduction (Sn_9^{4-}, Bi_4^{2-}, *etc.*) are fairly familiar or at least 'friendly' as they all follow modified rules for skeletal electron counts as outlined by Wade, Mingos, *etc.* But only a few such examples are found in 'neat' systems with the active metals. Those among the tetrel elements Si to Pb (recently reviewed[47]) are principally the tetrahedral anions in phases such as KSi, dimers in $BaMgSi_2$ and the like, an equal number of dimers and monomers in Ca_5Si_3, *etc.* (Cr_5B_3 type), and only monomers in Ca_2Si. It should be noted that the oxidation states in the respective Si_4^{4-}, Si_2^{6-} and Si^{4-} units make them isoelectronic and isosteric with P_4, Cl_2 and Ar. These are classic Zintl phases, basically obeying octet valence rules as judged structurally.[4,48] Many more examples can be found among network structures, including some structurally rather complex ways of fulfilling octet rules. In $CaGe_2$ complete electron transfer would yield Ge^- which is electronically equivalent to elemental As and, indeed, the structure contains As-like layers of three-bonded (3b-) Ge^- separated by the cations. Although the isostructural analogues Ca_2Sn and $CaSn_2$ are formally intermetallic phases, they are far removed from the traditional characteristics of such materials. The large differences in valence energies of the components afford substantial electron transfer and closed-shell covalent substructures for the anionic lattice, if any. (Actual charges on these ions are certainly not as extreme as the oxidation states, which are generally intended.) The inferred closed-shell character also implies that Zintl phases are semiconductors (or semimetals), but these aspects have been examined only in a few cases.

Clusters of Triel Elements

A cluster chemistry among alkali-metal compounds of the triel elements Al to Tl is both unexpected and unpredictable, and until 1991 only one example was known, the tetrahedral anion in Na_2Tl. Several factors had presumably generated skepticism, or at least an unconscious disbelief, concerning the existence of a significant chemistry, especially for In and Tl. (This is often a poor reason for not doing the experiments.) The electron affinities and presumably metal–metal bond strengths are expected to decrease down the group. In addition, classical deltahedral clusters if formed would necessarily have relatively high negative charges and high polarizability by cations, *e.g.* *closo*-M_n^{-n-2} with $2n + 2$ skeletal (p) electrons plus n additional pairs lying lower in predominantly s-based MOs. By contrast, the borane(2−) analogues have n protons of constitution, a bonding situation that is unlikely for its heavier congeners.

In fact, the trends down the boron group are not altogether so simple. Elemental boron and borides exhibit a rather distinctive, complex chemistry, featuring icosahedra and their fragments along with a few traditional Zintl phases (CaB_6, MgB_2, CrB).[49] Aluminium produces very few straightforward examples; compounds in which it is a dominant member exhibit a rather different complex chemistry without simple cluster units and plain relationships to Zintl phases.[50] Gallium does give strong hints of a significant chemistry *via* covalent Ga–Ga bonding in many network structures, usually constructed through interbonding of recognizable clusters.[51] Indeed, a recent interpretation of the unusual structure of elemental gallium, with one distinctively shorter bond, is in terms of cluster-like associations,[52] but until recently no isolated units were known. The surprises start with indium, which even in simple alkali-metal systems affords a mix of clusters in both network and discrete examples and the best examples of heterometal-centred clusters, while thallium shows a dominance of isolated clusters, icosahedra included, plus a few novel networks. The series reflects a trend from short, strong, and often localized bonds to more diffuse orbitals, more metal-like behaviour and longer, weaker bonds. The metal–metal bond strengths must still be significant in the many cluster species to be considered; these obviously remain competitive with the alternative phases, the alkali metals and the triel elements themselves which would generally not be regarded as strongly bonded. The particularly abrupt differences between aluminium

and gallium in their cluster chemistry are paralleled by several changes in fundamental properties, which are generally attributed to the intrusion of the 3d elements just preceding Ga and to the incomplete shielding of the extra nuclear charges provided by the 3d electrons.[53]

Zintl phases that contain nominally isolated trielide clusters will be considered first as these in principle involve the simpler electronic assessments. The fifteen or so examples of cluster types are rather recent discoveries, largely only because of a lack of looking, it appears. It is not possible to consider these in much detail here (a review is in progress[47]). However, some new and general lessons will be illustrated: ways in which simple, naked closed-shell clusters can be achieved in the hypoelectronic regime (relative to classical skeletal counting) through either distortion or centring, and how compounds containing new clusters may be tuned *via* the use of mixed cations. Formal anions of these elements are naturally very good reducing agents.

Homoatomic clusters

Twelve types of isolated homoatomic clusters are now known, increasing in frequency and variety from Ga to In to Tl. The nine larger examples are listed in Table 2 along with some note of their symmetries, while illustrations of Tl_5^{7-}, Tl_6^{6-}, Tl_9^{9-}, In_{11}^{7-}, $Tl_{12}(Na)^{13-}$ and Tl_{13}^{11-} appear in Fig. 13. There is no doubt that more will be found when the selection of cations is varied more widely. All but the A_8M_{11} (M = triel element) and $Na_4A_6Tl_{13}$ families are structurally correct Zintl phases, although the delocalization of a few valence electrons to give metallic conduction in what can be called *metallic Zintl phases* appears pertinent in other compounds. Four of the smaller cluster types with higher assigned charges (more negative oxidation states) per atom are also classic closed-shell ions, *nido*-M_4^{8-} (compare Sn_4^{4-}), *nido*-In_5^{9-}, *closo*-Tl_5^{7-} ($\hat{=}$ Pb_5^{2-}[5]) and *closo*-M_6^{8-}.

The clusters Tl_6^{6-} and In_{11}^{7-} afforded the first examples of simple hypoelectronic clusters achieved *via* distortions that empty one MO that was bonding in the ideal cluster. In CsTl [Fig. 13(*b*)] a tetragonal compression (Jahn–Teller distortion) of the classical octahedral Tl_6^{8-} empties one-third of the apex–waist t_{1u} MOs, leaving the cluster Tl_6^{6-} with $2n$ rather than $2n + 2$ skeletal bonding electrons (generally the $6s^2$ on each Tl are substantially core states). (The undistorted Ga_6^{8-} and Tl_6^{8-} subsequently turned up in ternary phases.) The other example is the relatively common M_{11}^{7-} cluster in the metallic salts $A_8M_{11}(e^-)$. The MO treatment for In_{11}^{7-} shown in Fig. 14 provides a good understanding of how a distortion can lead to these electron-poor clusters.[58] The starting 11-atom ideal on the left can be derived from the (hypothetical) *closo* tricapped-trigonal-prismatic In_9^{11-} through capping with two In^+ ions along the three-fold axis, which process introduces no new bonding orbitals or skeletal electrons and gives In_{11}^{9-}. As shown on the right, the observed axial compression yields In_{11}^{7-} as it (*a*) opens up the In(3) basal faces of the trigonal prism, and (*b*) yields additional bonding between each end-capping In(1) and the three waist-capping In(2) atoms, these driving the respective a_1'' MO higher while decreasing the energy of the pertinent a_1' and e′ MOs.

The strong influence of the cation packing around these naked clusters, such that the M_{11}^{7-} structure requires one extra alkali-metal atom per cluster, has become a recognizable feature of these compounds. (The isomorphous substitution product $K_8In_{10}Hg$ is properly diamagnetic.[63]) Further evidence of packing effects is seen in the significant number of other clusters that have been obtained only with mixtures of alkali-metal cations, but not from binary A–M systems. Five examples appear in Table 2. The cations inevitably exhibit specific roles about the deltahedral anions, capping triangular faces, bridging edges, bonding *exo* at metal vertices, and generally playing dual roles in bridging between clusters. The packing in the $Na_4A_6Tl_{13}$ structure is so tight and specific that only 10 cations per cluster can be accommodated, leaving a highly unusual one-electron hole in the Tl_{13}^{10-} anion, the opposite of the effect evidently responsible for the extra A element in the A_8M_{11} phases. So far, only the composition $Na_3K_8Tl_{13}$ has been found to yield the closed shell Tl_{13}^{11-}, an anion that can be easily generated conceptually by centring the

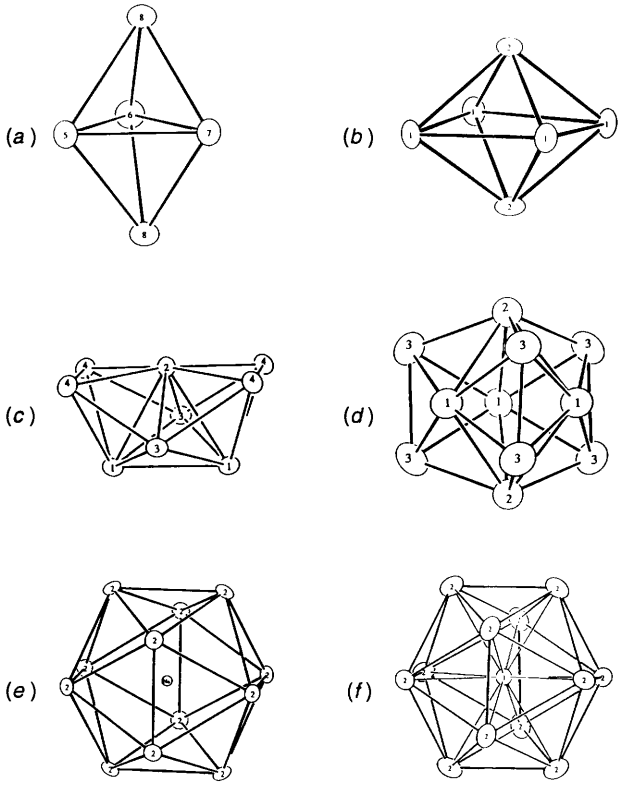

Fig. 13 Some trielide cluster anions with multicentre bonding: (*a*) Tl_5^{7-}, (*b*) Tl_6^{6-} ($\approx D_{4h}$), (*c*) Tl_9^{9-}, (*d*) In_{11}^{7-} ($\approx D_{3h}$), (*e*) $Tl_{12}(Na)^{13-}$ (T_h), (*f*) Tl_{13}^{10-} (T_h). Geometric tie-lines, not bonds, are shown. See Table 2 for the corresponding phase compositions

Table 2 Some homoatomic cluster anions of Ga, In, Tl (M) in Zintl phases

Ion	M Members	Symmetry[a]	Compound example	Ref.
M_4^{8-}	In, Tl	T_d (*nido*)	Na_2In	54
Tl_5^{7-}		$\approx D_{3h}$	$Na_2K_{21}Tl_{19}$	55
In_5^{9-}		C_{4v} (*nido*)	La_3In_5	56
Tl_6^{6-}		D_{4h}	CsTl	57
M_6^{8-}	Ga, Tl	O_h	$Na_{14}K_6Tl_{18}Mg$, $Ba_5Ga_6H_2$	57, 58
Tl_9^{9-}		C_{2v} (defect I_h)	$Na_2K_{21}Tl_{19}$	55
M_{11}^{7-}	Ga, In, Tl	$\approx D_{3h}$	A_8M_{11},[b] A = K to Cs	59–61
Tl_{13}^{10-}		T_h ($\approx I_h$)	$Na_4Rb_6Tl_{13}$	62
Tl_{13}^{11-}		D_{3h} ($\approx I_h$)	$Na_3K_8Tl_{13}$	62

[a] *closo* unless noted otherwise. [b] Contains an extra electron; not a classic Zintl phase.

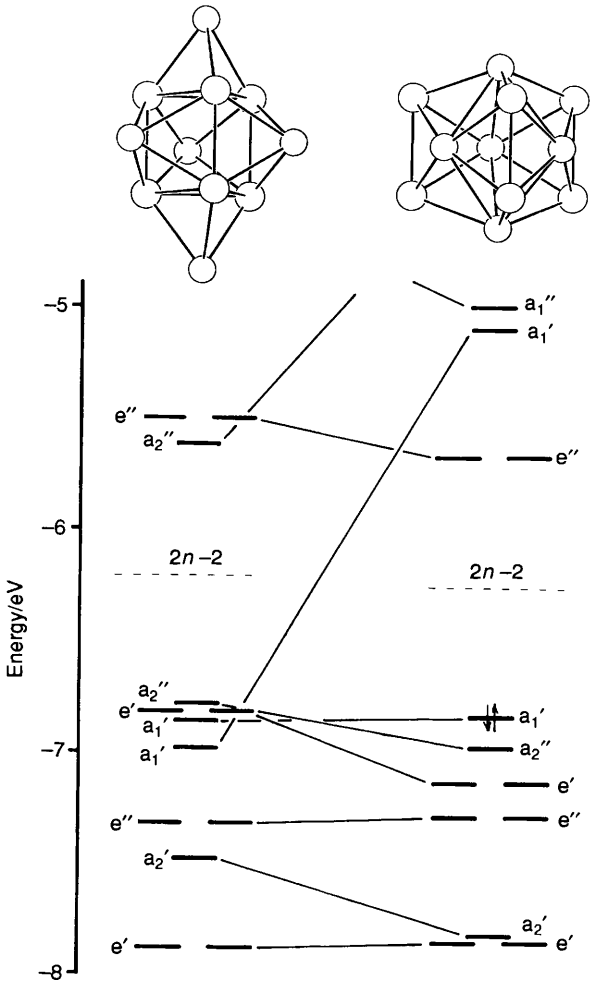

Fig. 14 Extended Hückel MO results for the hypoelectronic In_{11}^{7-}. Left: the scheme for a classical tricapped trigonal prism that has been further capped along the vertical three-fold axis. Right: the observed result after compression and lateral expansion to the observed polyhedron with $2n - 4$ skeletal bonding electrons

normal *closo*-Tl_{12}^{14-} with Tl^{3+}. The unusual closed-shell Tl_9^{9-} [Fig. 13(*c*)] follows directly from Tl_{13}^{11-} [Fig. 13(*f*)] on removal of four adjoining vertices and two skeletal electrons.

There is compelling evidence for the persistence of deltahedral clusters in liquid alloys, KTl for instance, and these seem to show some remarkable intercluster order as well.[64] It is imagined that many cluster species are potentially available in the liquids, and those that fractionate into a particular crystalline solid depend very much on the attainment of a suitable packing with, and sheathing and bridging by, the cations.

Heterometallic clusters

The triel clusters also demonstrate a remarkable parallel with centred cluster halides described in the first part of this Perspective, in this case incorporating interstitial elements that afford central bonding, distortions that lead to hypoelectronic regimes and, for some, additional electrons to fill the bonding manifold. Five examples of this as well as a substitution variant are summarized in Table 3. Fig. 15 shows two centred members, $In_{10}Zn^{8-}$ and $In_{10}Ni^{10-}$, together with the unusual substitution result $Tl_9Au_2^{9-}$. The first allows a simpler bonding consideration because of its higher symmetry, D_{4h}. The energetics of the centring process, as deduced from charge-consistent extended-Hückel calculations,[66] start with the traditional bicapped square antiprism. Compression along the four-fold axis and lateral expansion to the observed geometry,

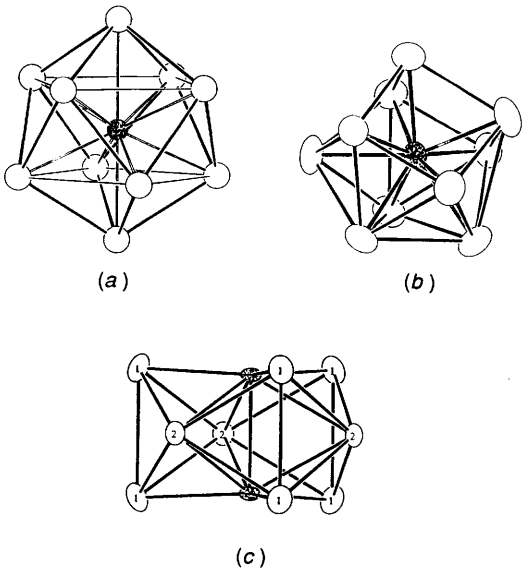

Fig. 15 Heteroatomic cluster anions (*a*) $In_{10}Zn^{8-}$ ($\approx D_{4h}$), (*b*) $In_{10}Ni^{10-}$ ($\approx C_{3v}$, axis vertical) and (*c*) $Tl_9Au_2^{9-}$ (D_{3h}). The heteroatoms are dotted

putting all vertices approximately equidistant from the centre, once again open up the capped faces and drive a former a_1 HOMO higher, leaving $2n$ skeletal electrons. The addition of a centred Zn atom with s and p valence orbitals and two s electrons generates good overlap with, and lowers the energy of, the four corresponding cluster-based MOs, driving another a_1 higher and leaving an e_3^4 HOMO for $2n = 20$ skeletal electrons.

The behaviour of the isoelectronic $In_{10}Ni^{10-}$ cluster, Fig. 15(*b*), is similar. The polyhedron is roughly a tetracapped trigonal prism ($\approx C_{3v}$) [compare In_{11}^{7-} in Fig. 13(*d*)] wherein only one basal face of the prism has been capped and opened up. Note the alternative configuration relative to that of the isoelectronic $K_8In_{10}Zn$, apparently because of the larger number of cations to be accommodated. The d levels of the transition metals in these highly reduced phases lie quite low and are not significantly involved in the cluster bonding, rather the interstitials Ni, Pd and Pt behave as quasi-main-group elements that are again bonded through valence s and p orbitals.[67] Finally, the $Tl_9Au_2^{9-}$ ion in the rather complex $K_{18}Tl_{20}Au_3$ derives directly from the closed-shell Tl_{11}^{7-} cluster [compare Figs. 13(*d*) and 15(*c*)]. Substitution of two Au atoms at the axial positions in Tl_{11}^{7-} is followed (in the mind) by a strong axial compression to yield a short (2.96 Å) Au–Au bond, for which the out-of-phase axial bonding a_2 MO in Tl_{11}^{7-} becomes Au–Au σ^* and empty. Thus, the addition of only two electrons yields closed-shell $Tl_9Au_2^{9-}$.

The magnetic and electronic properties of these cluster phases offer some useful insights into what is important in properties and what should be called Zintl phases.[47] A good number of the indium and thallium cluster phases are diamagnetic, although they may still show high but metal-like resistivities ($\geqslant 200$ μΩ cm). Even more important are those that are structurally Zintl-like but show Pauli-like (conduction electron) paramagnetism as well, *i.e.* metallic Zintl phases.[70] The compound La_3In_5 is a good example because the well defined square pyramids strongly implicate an electron-precise *nido*-In_5^{9-} therein. With relatively few cations, the separations between In_5^{9-} anions is not very large relative to the average within these (by 11%, 0.23 Å), and some evident delocalization (banding) of the higher-lying cluster electrons must occur, aided by the high-field La^{3+}. This should not detract from, let alone negate, the chemical insights gained from recognition of the In_5^{9-} clusters therein. This is even more emphatic for those phases which, evidently for packing (solvation) reasons, require extra alkali-

Table 3 Centred heteroatomic (*closo*) clusters of Ga, In, Tl in Zintl phases

Ion	M,M′ Range	Symmetry	Sample compound	Ref.
Tl_8H^{7-}		D_{3h}	$Na_{15}K_6Tl_{18}H$	65
$M_{10}Zn^{8-}$	In, Tl	D_{4d}	$K_8In_{10}Zn$	66
$M_{10}M'^{10-}$	Ga to Tl; Ni to Pt	$\approx C_{3v}$	$K_{10}In_{10}Ni$	57,67,68
$Tl_9Au_2^{9-a}$		D_{3h}	$K_{18}Tl_{20}Au_3$ [b]	69
$Tl_{12}Na^{13-}$		T_h	$Na_{15}K_6Tl_{18}H$	65
$Tl_{12}M'^{12-}$	Mg, Zn, Cd, Hg	T_h	$Na_{14}K_6Tl_{18}Mg$	57

[a] Substitutional derivatives of Tl_{11}^{7-}. [b] Contains an extra lattice electron; a metallic Zintl phase.

metal atoms, A_8M_{11}, $K_{18}Tl_{20}Au_3$ and some network structures, to follow. In some more classically bonded but electron-deficient structures one can imagine that formal electron pairs are lost (lie above E_F), *i.e.* on 3b-In^{2-} (-In-), 2b-In^{3-} (-In-), *etc.*

Triel networks

Extended structures of the triels Ga, In and Tl afford striking demonstrations of how complex compositions and structures may become in apparent response to valence demands and in order to meet, or approach, Zintl phase (closed-shell) conditions. There are in addition a few fairly simple but useful illustrations, starting with those that are electronically derivatives of the allotropes of carbon.[4] The isostructural LiAl, LiGa, LiIn, NaIn and NaTl (NaTl-type) consist of a cation-stuffed diamond lattice of Tl^-, *etc.* (or two interpenetrating diamond lattices). Size proportions clearly limit these to the smaller alkali metals. The group is sometimes categorized as *the* Zintl phases, and they are probably the best characterized.[71] The closely related LiAlSi and so forth amount to a cubic zinc blende lattice with half the octahedral cavities occupied by Li. A large group with $CaIn_2$ as the parent structure may be viewed as stuffed hexagonal diamond, or as stuffed wurtzite when the network atoms are distinguishable and alternate, in LiGaGe and NaInSn for instance. When the cations become large relative to the triel element, the layers separate and become planar in what is familiarly known as an AlB_2 (or inverse Ni_2In) type, an intercalated graphite analogue that is formally a Zintl phase for $CaGa_2$, *etc.*

A considerable number of alkali metal–triel phases are constructed from interbonded deltahedral clusters that are best described individually with delocalized bonding pictures. The intercluster bonds are apparently normal 2c–2e (two centre–two electron) types and can be thought to result following a one-electron oxidation of the s pair at each interbonded vertex (plus some rehybridization), so that each *exo* bond formed reduces the charge on each cluster by one.[51,72] A simple version is found for Rb_2In_3, *etc.*, in which standard In_6^{8-} octahedral clusters are joined into two-dimensional infinite square nets through formation of four equatorial bonds about each, as shown in Fig. 16.[73] The bridge bonds are 0.21 Å shorter than the average within the octahedra. Similarly, the ideal *closo*-M_{12}^{14-} icosahedra become M_{12}^{2-} when all vertices are bonded to 12 other clusters or bridging atoms, as occurs in Li_2Ga_7 (Li_4Ga_{14}) in which Ga_{12}^{2-} icosahedra are so interconnected *via* two 4b-Ga^- (equivalent to Ge^0). The utility of the foregoing ideas is clearly attested to by the frequent occurrence of such 'building blocks' in apparently valence-precise network structures.[47,51,74]

There are, of course, also other networks that only approach a match between the electron requirements of the framework and those available from the cations. In the $Na_7In_{11.76}$ phase, for instance, which contains the novel *closo*-In_{16} icosiocta-hedron plus *nido*-In_{11} and *arachno*-In_{10} in 5:3 proportions, is calculated to require 504 electrons per cell (with s cores), and 507 e^- are available on the basis of the refined structure.[75] Another compound that illustrates other novel bonding features is $Rb_3Na_{26}In_{48}$ represented in Fig. 17.[76] Here interbonded *closo*-icosahedra and *arachno*-In_{12} 'drums' gener-

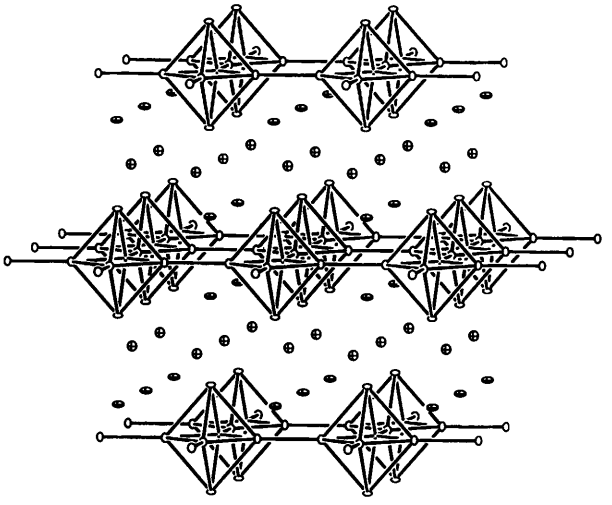

Fig. 16 The network structure of Rb_2In_3 with the $^2_\infty[In_6^{4-}]$ nets outlined. Isolated units are cations. Reprinted with permission from ref. 73

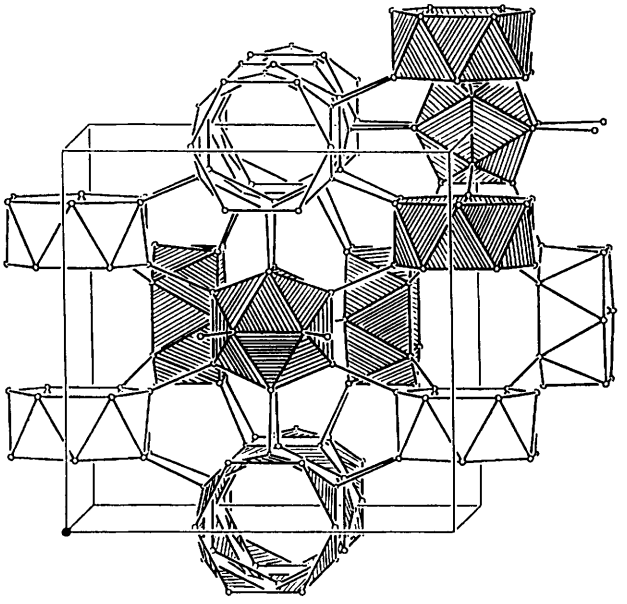

Fig. 17 The In_{12} drums and In_{12} icosahedra in $Rb_3Na_{26}In_{48}$. The cations have been omitted

ate an array of clusters that are centred about the atom positions of the simple A15 (Cr_3Si) structure. The small proportion of a larger cation (K, Rb or Cs) is evidently required to fill the large cavities between the In_{12} drums, and in this case there are 5.5% excess (metallic) electrons. There are many other gallium and a few indium cluster network compounds of this character. The evident drive to fulfil valence needs in such three-dimensional structures is of course greatly complicated by obvious structural requisites: relatively good space-filling

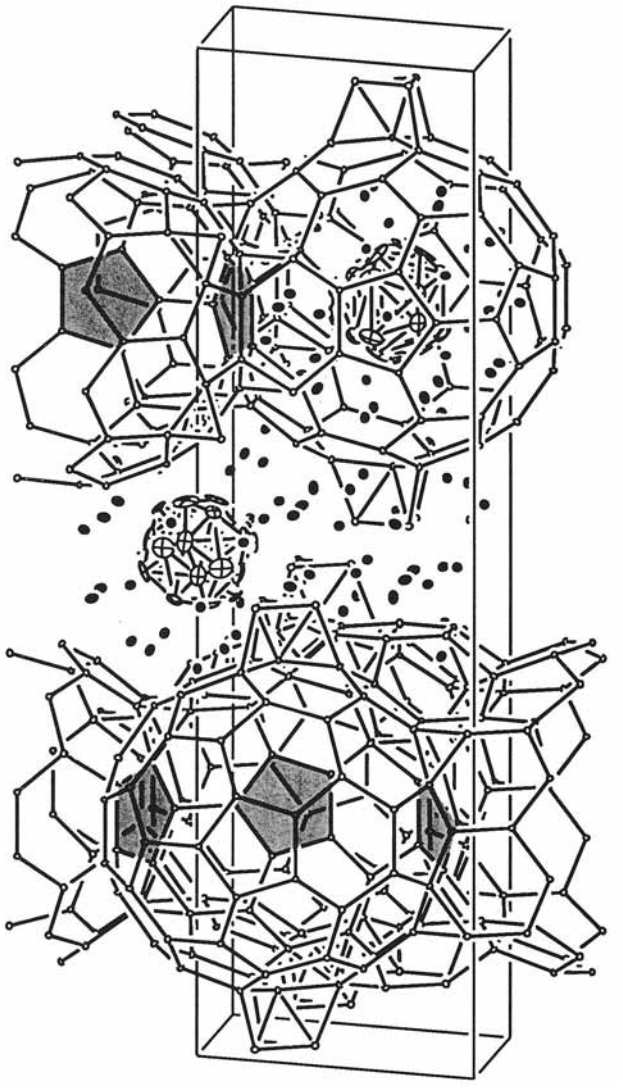

Fig. 18 Two layers of condensed, close-packed cages in $Na_{96}In_{97}Ni_2$. The bottom portion illustrates the condensation of In_{74} units through shaded pentagonal faces plus the surface decorations near the poles, while the cation positions and the interlayer and intracage (partially disordered) $In_{10}Ni$ cores are included in the upper part. Sodium lies inside and outside of each face of the In_{74} buckyballs. Reprinted with permission from *Science*, ref. 77. Copyright 1993 American Association for the Advancement of Science

efficiency from large clusters (and spacers) plus the appropriate and necessary intercluster bonding, and room for whatever cations are required, all in a relatively well ordered crystal. The strength and importance of homoatomic bonding for anionic states of the triels is especially impressive.

I close with an indium example that exhibits another step forward in complexity and beauty, but a step backwards in our ability readily to understand details of bonding and properties. Such characteristics pertain to two 'carbon-free fullerenes' of indium.[77] The essence of the simpler of these, $Na_{96}In_{97}Z_2$ (Z = Ni, Pd or Pt), is shown in Fig. 18 for Z = Ni. The basic component is a In_{74} 'buckyball' with the requisite 12 pentagonal faces that has been condensed, stuffed and 'decorated'. Indium is not effective at π bonding, and so each three-bonded vertex in an isolated In_{74} gains at least one more neighbour by some means (and so the compounds are probably better called 'fulleranes'[78]). Six pentagons around the waist of each In_{74} (D_{3h} symmetry) are shared with like faces on neighbouring cages (shaded in the figure) to generate close-packed layers. Cage atoms nearer the poles gain additional In–In bonding from added indium in triangular and hexagonal decorations ('warts'). The multiply endohedral or onion-like construction of these spheres is a particularly striking feature.

As shown only in the upper layer, Fig. 18, each large In_{74} unit contains a Na_{39} polyhedron in a duality role such that a cation falls inside (and outside) of every face of the cage. Within the sodium polyhedra there is in turn a partially disordered In_{10} unit that is centred by a single Ni atom, this group being very similar (if not identical) to that known separately in $K_{10}In_{10}Ni$ [Fig. 15(*b*)]; hence, the shell description $Ni@In_{10}@Na_{39}@In_{74}$ (@ represents 'within'). This and a second more complex phase $Na_{172}In_{199}Ni_2$ both feature additional $Ni@In_{10}@Na_{32}@(Na_{12}In_{48})$ cages (seen here between the layers) plus a $Ni@In_{10}@Na_{37}@In_{70}$ polycluster in the latter.[79] A portion of the latter is shown on the front cover. Notice that $Na_{96}In_{97}Z_2$ is, without the Z core, extremely close in composition and electron count to NaIn (NaTl-type) in which $In^- \triangleq C^0$, Si^0, *etc.* Nesper[78] has described a few other endohedral fullerane examples, including some older types in which the polyhedra do not occur as simple building blocks. Not surprisingly, aluminium forms some of the closest analogues.

It all comes from synthetic curiosity and luck.

Acknowledgements

The graduate students and postdoctoral associates whose names appear in the references deserve much of the credit for the science that is described here. This cluster halide research has been supported by the National Science Foundation, Solid State Chemistry, *via* Grant DMR-9207361 (and earlier grants). The main-group cluster and Zintl phase program has been sponsored by Basic Energy Sciences, Materials Sciences Division, U.S. Department of Energy (DOE), and both were carried out in the Ames Laboratory-DOE. Ames Lab is operated for DOE by Iowa State University under Contract No. W-7405-Eng-82.

References

1 H. Schäfer and H.-G. Schnering, *Angew. Chem.*, 1964, **76**, 833.
2 A. F. Wells, *Structural Inorganic Chemistry*, 5th edn., Clarendon Press, Oxford, 1984, ch. 9.
3 J. Köhler, G. Svensson and A. Simon, *Angew. Chem., Int. Ed. Engl.*, 1992, **31**, 1437; J. Köhler and A. Simon, *Z. Anorg. Allg. Chem.*, 1989, **572**, 7; R. Dronskowski, A. Simon and W. Mertin, *Z. Anorg. Allg. Chem.*, 1991, **602**, 49.
4 H. Schäfer, *Annu. Rev. Mater. Sci.*, 1985, **15**, 1.
5 J. D. Corbett, *Chem. Rev.*, 1985, **85**, 383.
6 J. D. Corbett, in *Solid State Chemistry: Techniques*, eds. A. K. Cheetham and P. Day, Clarendon Press, Oxford, 1987, ch. 1, pp. 1–38.
7 F. Böttcher, A. Simon, R. K. Kremer, H. Buchkremer-Hermanns and J. K. Cockcroft, *Z. Anorg. Allg. Chem.*, 1991, **598/599**, 25.
8 F. A. Cotton and W. A. Wojtczak, *Inorg. Chim. Acta*, 1994, **223**, 93.
9 R. P. Ziebarth and J. D. Corbett, *Acc. Chem. Res.*, 1989, **22**, 256.
10 J. D. Corbett, *Modern Perspectives in Inorganic Crystal Chemistry*, ed. E. Parthé, Kluwer Academic Publishers, Dordrecht, 1992, p. 27.
11 A. Simon, Hj. Mattausch, G. J. Miller, W. Bauhofer and R. K. Kremer, in *Handbook on the Physics and Chemistry of Rare Earths*, eds. K. A. Gschneidner and L. Eyring, Elsevier, Amsterdam, 1992, vol. 15, p. 191.
12 J. D. Corbett, *J. Alloys Compd.*, 1995, **229**, 10.
13 J. D. Corbett and R. E. McCarley, in *Crystal Chemistry and Properties of Materials with Quasi-One-Dimensional Structures*, ed. J. Rouxel, D. Reidel, Dordrecht, 1986, pp. 179–204.
14 J. D. Martin and J. D. Corbett, *Angew. Chem., Int. Ed. Engl.*, 1995, **34**, 233.
15 J. D. Smith and J. D. Corbett, *J. Am. Chem. Soc.*, 1985, **107**, 5704.
16 R. P. Ziebarth and J. D. Corbett, *J. Am. Chem. Soc.*, 1985, **107**, 4571.
17 M. Köckerling, R.-Y. Qi and J. D. Corbett, *Inorg. Chem.*, 1996, **35**, in the press.
18 J. Zhang and J. D. Corbett, *Inorg. Chem.*, 1991, **30**, 431.
19 R.-Y. Qi and J. D. Corbett, *Inorg. Chem.*, 1995, **34**, 1646, 1657.
20 J. Zhang and J. D. Corbett, *Inorg. Chem.*, 1995, **34**, 1652.
21 R.-Y. Qi and J. D. Corbett, unpublished work.
22 G. Rosenthal and J. D. Corbett, *Inorg. Chem.*, 1988, **27**, 53.
23 R.-Y. Qi and J. D. Corbett, *Inorg. Chem.*, 1994, **33**, 5727.

24 D. J. Hinz and G. Meyer, *J. Chem. Soc., Chem. Commun.*, 1994, 125.
25 T. Hughbanks, G. Rosenthal and J. D. Corbett, *J. Am. Chem. Soc.*, 1988, **110**, 1511.
26 T. Hughbanks, *Prog. Solid State Chem.*, 1989, **19**, 329.
27 J. D. Corbett, *J. Solid State Chem.*, 1981, **37**, 335.
28 R. P. Ziebarth and J. D. Corbett, *J. Am. Chem. Soc.*, 1989, **111**, 3272.
29 H. Imoto, J. D. Corbett and A. Cisar, *Inorg. Chem.*, 1981, **20**, 145.
30 J. Zhang, R. P. Ziebarth and J. D. Corbett, *Inorg. Chem.*, 1992, **31**, 614.
31 P. J. Chu, R. P. Ziebarth, J. D. Corbett and B. C. Gerstein, *J. Am. Chem. Soc.*, 1988, **110**, 5324.
32 J. D. Corbett, J. Eckert, U. A. Jayasooriya, G. J. Kearley, R. P. White and J. Zhang, *J. Phys. Chem.*, 1993, **97**, 8384.
33 F. Rogel and J. D. Corbett, *J. Am. Chem. Soc.*, 1990, **112**, 8198; F. Rogel, J. Zhang, M. W. Payne and J. D. Corbett, *Adv. Chem. Ser.*, 1990, **226**, 369.
34 C. E. Runyan, jun., and T. Hughbanks, *J. Am. Chem. Soc.*, 1994, **116**, 7909; Y. Tian and T. Hughbanks, *Inorg. Chem.*, 1995, **34**, 6250; T. Hughbanks, *J. Alloys Compd.*, 1995, **229**, 4001.
35 T. Hughbanks and J. D. Corbett, *Inorg. Chem.*, 1989, **28**, 631.
36 R. Llusar and J. D. Corbett, *Inorg. Chem.*, 1994, **33**, 1705.
37 M. W. Payne and J. D. Corbett, *Inorg. Chem.*, 1990, **29**, 2246.
38 Y. Park and J. D. Corbett, *Inorg. Chem.*, 1994, **33**, 1705.
39 M. W. Payne, M. Ebihara and J. D. Corbett, *Angew. Chem., Int. Ed. Engl.*, 1991, **30**, 856.
40 S. J. Steinwand and J. D. Corbett, unpublished work.
41 M. Ebihara, J. D. Martin and J. D. Corbett, *Inorg. Chem.*, 1994, **33**, 2079.
42 M. W. Payne, P. K. Dorhout and J. D. Corbett, *Inorg. Chem.*, 1991, **30**, 1467.
43 S. M. Kauzlarich, T. Hughbanks, J. D. Corbett, P. Klavins and R. N. Shelton, *Inorg. Chem.*, 1988, **27**, 1791.
44 M. W. Payne, P. K. Dorhout, S.-J. Kim, T. R. Hughbanks and J. D. Corbett, *Inorg. Chem.*, 1992, **31**, 1389.
45 P. K. Dorhout and J. D. Corbett, *J. Am. Chem. Soc.*, 1992, **114**, 1697.
46 K. Ahn, T. Hughbanks, K. D. D. Rathnayaka and D. G. Naugle, *Chem. Mater.*, 1994, **6**, 418.
47 J. D. Corbett, in *Chemistry, Structure and Bonding of Zintl Phases and Ions*, ed. S. Kauzlarich, VCH.
48 T. Hughbanks, in *Inorganometallic Chemistry*, ed. T. Fehlner, Plenum, New York, 1992, p. 291.
49 A. F. Wells, *Structural Inorganic Chemistry*, 5th edn., Clarendon Press, Oxford, 1984, p. 1049.
50 R. Nesper, *Angew. Chem., Int. Ed. Engl.*, 1991, **30**, 789.
51 C. Belin and M. Tillard-Charbonnel, *Prog. Solid State Chem.*, 1993, **22**, 59.
52 H.-G. von Schnering and R. Nesper, *Acta Chem. Scand.*, 1991, **45**, 870.
53 N. N. Greenwood and A. Earnshaw, *Chemistry of the Elements*, Pergamon, Oxford, 1984, p. 250.
54 S. C. Sevov and J. D. Corbett, *J. Solid State Chem.*, 1993, **103**, 114.
55 Z.-C. Dong and J. D. Corbett, *J. Am. Chem. Soc.*, 1994, **116**, 3429.
56 J.-T. Zhao and J. D. Corbett, *Inorg. Chem.*, 1995, **34**, 378.
57 Z.-C. Dong and J. D. Corbett, unpublished work.
58 Q. Liu, R. Hoffmann and J. D. Corbett, *J. Phys. Chem.*, 1994, **98**, 9360.
59 S. C. Sevov and J. D. Corbett, *Inorg. Chem.*, 1991, **30**, 4875.
60 W. Blase and G. Cordier, *Z. Kristallogr.*, 1991, **194**, 150.
61 Z.-C. Dong and J. D. Corbett, *J. Cluster Sci.*, 1995, **6**, 187.
62 Z.-C. Dong and J. D. Corbett, *J. Am. Chem. Soc.*, 1995, **117**, 6447.
63 S. C. Sevov, J. D. Corbett and J. E. Ostenson, *J. Alloys Compd.*, 1993, **202**, 289.
64 R. Xu, P. Verkerk, W. S. Howells, G. A. de Wijs, F. van der Horst and W. van der Lugt, *J. Phys.: Condensed Matter*, 1993, **5**, 9253.
65 Z.-C. Dong and J. D. Corbett, *Inorg. Chem.*, 1995, **34**, 5709.
66 S. C. Sevov and J. D. Corbett, *Inorg. Chem.*, 1993, **32**, 1059.
67 S. C. Sevov and J. D. Corbett, *J. Am. Chem. Soc.*, 1993, **115**, 9089.
68 R. Henning and J. D. Corbett, unpublished work.
69 Z.-C. Dong and J. D. Corbett, *Inorg. Chem.*, 1995, **34**, 5042.
70 R. Nesper, *Prog. Solid State Chem.*, 1990, **20**, 1.
71 P. C. Schmidt, *Struct. Bonding (Berlin)*, 1987, **65**, 91.
72 J. K. Burdett and E. Canadell, *J. Am. Chem. Soc.*, 1990, **112**, 7207.
73 S. C. Sevov and J. D. Corbett, *Z. Anorg. Allg. Chem.*, 1993, **619**, 128.
74 H. Schäfer, *J. Solid State Chem.*, 1985, **57**, 97.
75 S. C. Sevov and J. D. Corbett, *Inorg. Chem.*, 1992, **31**, 1895.
76 S. C. Sevov and J. D. Corbett, *Inorg. Chem.*, 1993, **32**, 1612.
77 S. C. Sevov and J. D. Corbett, *Science*, 1993, **262**, 880.
78 R. Nesper, *Angew. Chem., Int. Ed. Engl.*, 1994, **33**, 843.
79 S. C. Sevov and J. D. Corbett, *J. Solid State Chem.*, submitted.

Received 17*th August* 1995; *Paper* 5/06743J